Synthesis and crystal structure determination of the new olivine-type compound $Mn_2Sn\square Se_4$

C. Chacón[a], P. Delgado-Niño[b], and G. E. Delgado[c,*]
[a]*Cátedras Conacyt-Instituto Mexicano del Petróleo, Centro de Tecnología para Aguas Profundas, Veracruz, México.*
[b]*Facultad de Ingeniería, Universidad Libre, Av. Cr 70 53-40, Bogotá, Colombia.*
[c]*Laboratorio de Cristalografía, Departamento de Química, Facultad de Ciencias, Universidad de Los Andes, Mérida 5101, Venezuela.*
[*]*e-mail: gerzon@ula.ve*

Received 8 June 2019; accepted 19 August 2019

The $Mn_2Sn\square Se_4$ compound, manganese tin selenide, was synthesized by the melt and annealing technique and its structure was refined by the Rietveld method using X-ray powder diffraction data. This compound crystallizes in the olivine-type structure with unit cell parameters $a = 12.9028(2)$ Å, $b = 7.9001(1)$ Å, $c = 6.5015(1)$ Å, $V = 662.72(2)$ Å^3 in the orthorhombic space group $Pnma$ (N° 62). This olivine structure can be described from a hexagonal close-packing of selenium atoms where manganese atoms occupy 1/2 of the octahedral sites while thin atoms lay in 1/8 of the tetrahedra.

Keywords: Olivines; chacogenides; semiconductors; chemical synthesis; crystal structure; X-ray powder diffraction; Rietveld refinement.

PACS: 61.05.cp; 61.50.Nw: 61.66.Fn; 61.40.b

DOI: https://doi.org/10.31349/RevMexFis.66.30

1. Introduction

Most semiconductor compounds crystallize in tetrahedral structures, where each atom has as its first neighbors four other atoms bonded by sp^3 hybrid orbitals placed at the vertices of a tetrahedron. For the formation of these bonds, an average number of four valence electrons per atom is necessary. However, some derived structures involve the orderly omission of atoms resulting in so-called defect or vacancy semiconductor compounds. In this type of structures, some atom has less than four neighbors, due to the presence of vacancies in the cationic sites [1]. Moreover, magnetic semiconducting compounds and alloys in which manganese is one of the component elements are of interest because of the large magneto-optical effects, which can occur in these materials [2]. These semimagnetic compounds can be obtained from the tetrahedrally coordinated II-VI semiconductors by replacing a fraction of cations, following the rules of adamantane compounds formation. According to these rules, the cation substitution is performed in such a way that an average number of four valence electrons per atomic site and eight as the value for the ratio valence electrons to anions is maintained. In particular, two possible families of the fourfold defect derivatives of the II-VI binary semiconductors exist; II-III_2-□-VI_4 and II_2-IV-□-VI_4, where □ represents the cation vacancy which is included to maintain the same number of cations and anions sites [1].

Materials with composition II_2-IV-□-VI-4 with II = Mn, Fe, IV = Si, Ge, Sn, VI = S, Se, Te can be useful for applications such as thermoelectrics [3-5], optoelectronics [6], spintronics and magnetic devices [7-9]. The presence of transition metal and chalcogenide elements provide unique interactions between electron spins, from the transition metal, and p-orbital electrons that contribute to modifying the physical properties of these materials, and increase their potential for

TABLE I. Crystallography parameters and Curie temperature reported for the Mn_2-IV-□-VI_4 (IV= Si, Ge, Sn; VI= S, Se, Te) system.

Compound	SG	a (Å)	b (Å)	c (Å)	V (Å^3)	Ref.	Θ (K)	Ref.
Mn_2SiS_4	*Pnma*	12.688 (2)	7.429 (2)	5.942 (1)	560.1 (2)	[14]	-200	[21]
Mn_2SiSe_4	*Pnma*	13.3066(8)	7.7780(5)	6.2451(3)	646.4(1)	[15]	-230	[15]
Mn_2GeS_4	*Pnma*	12.776	7.441	6.033	573.53	[16]	-373	[22]
Mn_2GeSev	*Pnma*	13.350(3)	7.765(2)	6.307(1)	635.8(3)	[17]	-240	[17]
Mn_2GeTe_4	*Pnma*	13.950(2)	8.115(1)	6.592(1)	746.2(2)	[18]	-375	[7]
Mn_2SnS_4	*Cmmm*	7.397(4)	10.477(7)	3.664(3)	284.0(1)	[19]	-463	[23]
Mn_2SnSe_4	*Pnma*	13.49	7.858	6.494	688.4	[11]	-	
	Pnma	12.9028(2)	7.9001(1)	6.5015(1)	662.72(2)	this work	-	
Mn_2SnTe_4	*Pnma*	14.020(2)	8.147(1)	6.607(1)	754.7(2)	[20]	- 300	[24]

different applications [10]. It is therefore of great interest to establish its crystal structures and investigate its fundamental properties in order to further the understanding of their physical properties, and increase their potential for different applications.

Regarding to one of the fundamental properties as is their magnetic behavior, Mn derivatives have been reported to have antiferromagnetism behavior with Curie temperatures shown in Table I. The magnetic properties of $Mn_2Sn\square Se_4$ have not as yet been reported.

These materials generally crystallize in the olivine structure type, as shown in Table I for Mn derivatives, with the VI anions forming a hexagonal close packing, and the cations in tetrahedral (IV) and octahedral (II) coordination.

Particularly for the ternary $Mn_2Sn\square Se_4$ a poor quality powder diffraction pattern is reported in the Powder Diffraction File PDF-ICDD (039-0879) [11], with cell parameters and space group as unique information. However, a search in the databases Inorganic Crystal Structure Database (ICSD) [12] and Springer Materials [13], where are reported complete structural studies, showed no entries for this compound.

Therefore, the present work reports the synthesis and structural characterization of the new olivine-type compound $Mn_2Sn\square Se_4$, included unit cell parameters, atomic coordinates, isotropic temperature factors and geometric parameter values (cation-anion bond and angles), from powder X-ray diffraction data.

2. Experimental

Polycrystalline sample of $Mn_2Sn\square Se_4$ was synthesized using the melt and annealing technique. Stoichiometric quantities of highly pure Mn, Sn and Se elements, with a nominal purity of at least 99.99% (Sigma-Aldrich), were charged in an evacuated quartz ampoule, previously subject to pyrolysis in order to avoid reaction of the starting materials with quartz. The fusion process, 14 days, was carried out into a furnace (vertical position) heated up to 1050°C. Then, the temperature was gradually lowered to 500°C. Finally, the furnace was turned off and the ingots were cooled to room temperature. Chemical composition of the resultant ingot was determined at several regions by energy dispersive spectroscopic (EDS) analysis using a JMS-6400 scanning electron microscope (SEM). Three different regions of the ingot were scanned, and the average atomic percentages are: Mn (14.3%), Sn (28.5%) and Se (57.2%), very close to the ideal composition 2 : 1 : 4. The error in standardless analysis was around 5%.

X-ray powder diffraction pattern was collected at room temperature, in a Panalytical X'pert diffractometer using CuKα radiation ($\lambda = 1.5418$ Å). A small quantity of the sample was ground mechanically in an agate mortar and pestle and mounted on a flat holder. The specimen was scanned from 10 to 80°2θ, with a step size of 0.02° and counting time of 20 s. Silicon (SRM-640) was used as an external standard. The Panaytical X'pert Pro analytical software was used to establish the positions of the peaks.

3. Results and Discussion

X-ray powder diffractogram of Mn_2SnSe_4 shows a single phase (Fig. 1). The 20 first measured reflections were completely indexed using the program DICVOL04 [25], which gave a unique solution in an orthorhombic cell with unit cell parameters $a = 12.895(1)$ Å, $b = 7.860(1)$ Å, $c = 6.478(1)$ Å. Systematic absence of analysis indicates a P-type cell, which suggested along with the sample composition and cell parameter dimensions that this material is isostructural with the olivine-type compounds, crystallizing in the orthorhombic space group *Pnma* (N° 62). The crystal structure refinement carried out by the Rietveld method [26] was performed

TABLE II. Rietveld refinement details for $Mn_2Sn\square Se_4$.

Chemical formula	$Mn_2Sn\square Se_4$	wavelength (CuKα)	1.5418 Å
Formula weight (g/mol)	544.43	data range 2θ(°)	10-80
a (Å)	12.9028(2)	step size 2θ(°)	0.02
b (Å)	7.9001(1)	counting time (s)	20
c (Å)	6.5015(1)	step intensities	4001
V (Å^3)	662.72(2)	Peak-shape profile	pseudo-voigt
Z	4	R_p (%)	5.5
Crystal system	orthorhombic	R_{wp} (%)	5.9
Space group	*Pnma* (N° 62)	R_{exp} (%)	5.0
dcalc (g/cm^{-3})	5.46	R_B (%)	4.8
Temperature (K)	298(1)	S	1.2

$R_{\text{exp}} = 100[(N-P+C)/\sum_w (y_{obs}^2)]^{1/2}$, $R_p = 100\sum|y_{obs}-y_{calc}|/\sum|y_{obs}|$, $R_{wp} = 100[\sum_w |y_{obs}-y_{calc}|^2/\sum_w |y_{obs}|^2]^{1/2}$, $S = [R_{wp}/R_{\text{exp}}]$, $R_B = 100\sum_k |I_k - I_{ck}|/\sum_k |I_k|$, $N-P+C$ is the number of degrees of freedom

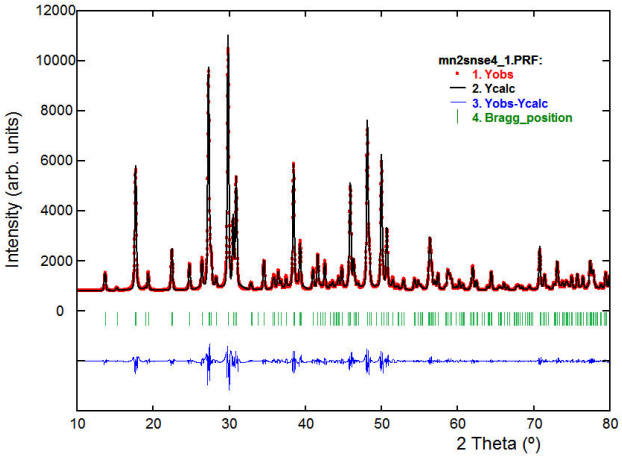

FIGURE 1. Observed, calculated, and difference plot of the final Rietveld refinement of $Mn_2Sn\square Se_4$. The Bragg reflections are indicated by vertical bars.

using the FULLPROF program [27], with the unit cell parameters obtained in the indexed. The atomic coordinates of the isomorphic compound Mn2SnTe4 [20] were used as starting parameters for the refinement. The instrumental and structural variables adjusted during the refinement were; zero shift, scale factor, asymmetry parameter, three pseudo-Voigt parameters of the peak-shape function, three unit cell parameters, eleven positional parameters and one overall isotropic temperature factor. The background was described by the automatic interpolation of 67 points throughout the whole pattern. The refinement converged to the final profile agreement factors summarized in Table II. Figure 1 shows the observed, calculated and difference profile for the final cycle of Rietveld refinement. Atomic coordinates, isotropic temperature factor, bond and angle distances are shown in Table III. Figure 2 show the unit cell diagram of Mn_2SnSe_4

Mn_2SnSe_4 crystallize in an olivine-type structure which consists of a three-dimensional arrangement of distorted $MnSe_6$ octahedra and $SnSe_4$ tetrahedra connected by common faces. The olivine structure can be described as a hexagonal close packing of Se^{-2} anions with the Mn^{+2} cations occupying half of the octahedral sites and the Sn^{+4} cations occupying an eighth of the tetrahedral sites. The Mn_1Se_6 octahedra are located at a center of symmetry and form infinite edge-shared chains parallel to [010]. In alternating positions to the left and right of the chains and situated half way between two Mn_1Se_6 octahedra, the Mn_2Se_6 octahedra are straddling the mirror planes perpendicular to [010]. The selenide ion common to the two octahedra $Mn-1Se_6$ and the Mn_2Se_6 octahedron forms one of the apices of an occupied $SnSe_4$ tetrahedron; the other 3 apices are located in a horizontal plane and are provided by 3 selenide ions of the chain below or above. Each Mn_1Se_6 octahedron shares: 2 edges with 2 Mn_1Se_6 octahedra, 2 edges with 2 Mn_2Se_6 octahedra, 2 edges with 2 $SnSe_4$ tetrahedra; while each Mn_2Se_6 octahe-

TABLE III. Atomic coordinates, occupancy factors, isotropic temperature factors and geometric parameters (Å, °) for $Mn_2Sn\square Se_4$.

Atom	Ox.	Site	x	y	z	foc	B_{iso} (Å^2)
Mn1	+2	$4a$	0	0	0	1	0.5(2)
Mn2	+2	$4c$	0.241(1)	1/4	0.503(1)	1	0.5(2)
Sn	+4	$4c$	0.404(1)	1/4	0.072(1)	1	0.5(2)
Se1	-2	$8d$	0.327(1)	0.007(1)	0.255(1)	1	0.5(2)
Se2	-2	$4c$	0.416(2)	1/4	0.689(2)	1	0.5(2)
Se3	-2	$4c$	0.583(2)	1/4	0.249(1)	1	0.5(2)

Mn1-Se1^{ii}	2.92(1)x2	Mn1-Se2^{iii}	2.66(1)x2	Mn1-Se3^{iv}	2.87(1)x2
Mn2-Se1^{v}	2.84(1)x2	Mn2-Se1	2.84(1)x2	Mn2-Se2	2.74(3)
Mn2-Se3^{iii}	2.77(3)				
Sn-Se1	2.56(1)x2	Sn-Se2i	2.54(2)	Sn-Se3	2.77(3)

Se1^{iv}-Mn1-Se2^{iii}	94.4(2)	Se1^{iv}-Mn1-Se3^{iv}	85.7(2)	Se1^{iv}-Mn1-Se3^{iii}	94.3(2)
Se1^{iv}-Mn1-Se2^{iv}	85.6(2)	Se1^{iv}-Mn1-Se1^{ii}	180.0(3)	Se2^{iii}-Mn1-Se2i^{v}	180.0(5)
Se3^{iv}-Mn1-Se3^{iii}	180.0(0)	Se1^{vi}-Mn2-Se1^{v}	174.9(2)	Se1-Mn2-Se1^{vii}	174.9(2)
Se3^{iii}-Mn2-Se2	171.9(7)	Se3^{iii}-Mn2-Se1^{vi}	88.3(2)	Se3^{iii}-Mn2-Se1	88.3(2)
Se3^{iii}-Mn2-Se1^{vii}	94.8(2)	Se3^{iii}-Mn2-Se1^{v}	94.8(2)	Se2^{i}-Sn-Se3	112.0(5)
Se2^{i}-Sn-Se1^{vi}	119.2(2)	Se2^{i}-Sn-Se1	119.2(2)	Se1^{vi}-Sn-Se3	100.9(3)
Se1^{vi}-Sn-Se1	101.9(3)	Se3-Sn-Se1	100.9(3)		

Symmetry codes: (i) $x, y, -1+z$; (ii) $-0.5+x, y, 0.5-z$; (iii) $-0.5+x, 0.5-y, 0.5-z$; (iv) $0.5-x, -y, -0.5+z$; (v) $0.5-x, -y, 0.5+z$; (vi) $x, 0.5-y, z$; (vii) $0.5-x, 0.5+y, 0.5+z$.

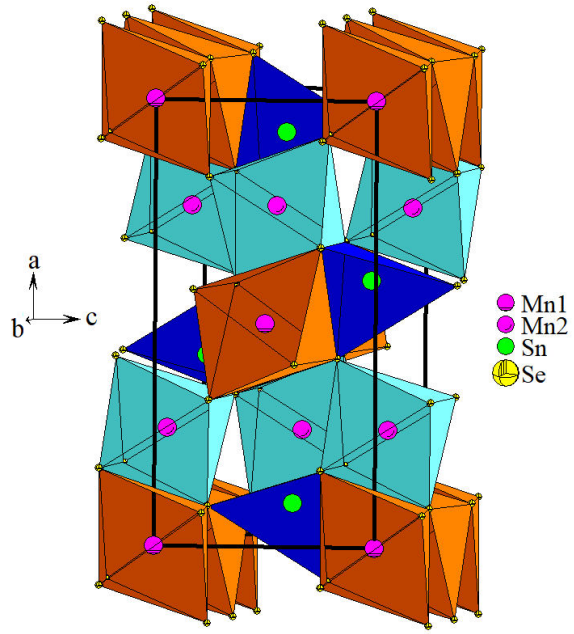

FIGURE 2. Unit cell diagram of the new olivine-type compound $Mn_2Sn\square Se_4$ ($Pnma$) showing the $MnSe_6$ octaedra and SnSe4 tetrahedra sharing faces in the crystal structure.

dron shares: 2 edges with 2 Mn_1Se_6 octahedra, 1 edge with 1 SnSe4 tetrahedron. Figure 2 shows how the octahedra and tetrahedra share faces.

The interatomic distances are shorter than the sum of the respective ionic radii for structures tetrahedrally bonded [28]. The Mn-Se [mean value 2.72(2) Å] and Sn-Se [mean value 2.53(2) Å] bond distances, compare well with the same distances found in related adamantane compounds such as Cu_2SnSe_3 [29], $CuMn_2InSe_4$ [30], $MnIn-2Se_4$ [31], $Cu_2MnSnSe_4$ [32] and the systems $CuGa_{(1-X)}Mn_{(X)}Se_2$ [33] and CuMn-III-Se_3 (III= Al, Ga, In) [34]. All of these phases were found in the Inorganic Crystal Structure Database (ICSD) [12].

4. Conclusions

The ternary compound $Mn_2Sn\square Se_4$ was synthesized and its crystal structure was determined using X-ray powder diffraction. This material crystallizes in the orthorhombic space group $Pnma$ with an olivine-type structure and corresponds with a new compound of the II-III_2-$\square$-VI_4 family with this crystalline arrangement.

Acknowledgments

This work was supported by FONACIT (Grant LAB-97000821).

1. E. Parthé, in *Intermetallic compounds, principles and applications*, edited by J. H. Westbrook and R. L. Fleischer (Wiley, Chichester, 1995), Vol. 1.
2. J. K. Furdyna and J. Kossut, in *Diluted magnetic semiconductors, in semiconductors and semimetals*, edited by R. K. Willardson and A. C. Beer (Academic, New York, 1988), Vol. 25.
3. V. K. Gudelli, V. Kanchana, and G. Vaitheeswaran, *J. Phys. Condens. Matter*. **28** (2016) 025502.
4. K. Wei, J. Martin, and G. S. Nolas, *J. Alloys Compd.* **732** (2018) 218e221.
5. H. Nagai, K. Hayashi, and Y. Miyazaki, *Trans. Mat. Res. Soc. Japan* **43** (2018) 13.
6. A. Davydova *et al.*, *Mater. Des.* **152** (2018) 110.
7. M. Quintero *et al.* , *J. Alloys Compd*. **469** (2009) 4.
8. M. Quintero *et al.*, *Magn. Magn.* **321** (2009) 291.
9. G. E. Delgado *et al.*, *Chalcogenide Letters*, **7** (2010) 133.
10. T. Jungwirth, J. Sinova, J. Mašek, J. Kučera, and A.H. MacDonald, *Rev. Mod. Phys*. **78** (2006) 809.
11. PDF-ICDD, *International Centre for Diffraction Data*, Newtown Square, PA, USA (2017).
12. ICSD, *Inorganic Crystal Structure Database*, Gemlin Institute, Kalrsruhe, Germany (2016).
13. Springer Materials, https://materials.springer.com (2019-06-06).
14. J. Fuhrmann, *J. Pickardt. Acta Cryst. C* **45** (1989) 1808.
15. S. Jobic, F. Bodénan, P. le Boterf, and G. Ouvrard, *J. Alloys Compd*. **230** (1995) 16.
16. M. Julien-Pouzol, S. Jaulmes, and S. Barnier, *J. Sol. State Chem.* **65** (1986) 280.
17. H. J. Deiseroth, K. Aleksandrov, and R. K. Kremer, *Z. Anorg. Allg. Chem*. **631** (2005) 448. (2005).
18. G. E. Delgado *et al.*, *Av. Quím.* **4** (2009) 7.
19. M. Wintenberger, and J. C. Jumas, *Acta Cryst. B* **36** (1980) 1993.
20. G. E. Delgado, A. J. Mora, J. E. Contreras, and L. Betancourt, *Bull. Mater. Sci.* **33** (2010) 247.
21. G. E. Delgado, A. J. Mora, J. E. Contreras, and L. Betancourt, *Bull. Mater. Sci*. **33** (2010) 247.
22. G. Lamarche, F. Lamarche, and A.-M. Lamarche, *Physica B*, **194-196** (1994) 219.
23. M. Partik, Th. Sting, H. D. Lutz, H. Sabrowsky, and P. Vogt, *Z. Anorg. Allg. Chem*. **621** (1995) 1600.
24. R. C. Haushalter, C. J. O'Connor, A. M. Umarji, G. K. Shenoy, and C. K. Saw, *Solid State Comm*. **49** (1984) 929.
25. A. Boultif, and D. Löuer, *J. Appl. Cryst*. **37** (2004) 724.
26. H. M. Rietveld, *J. Appl. Cryst*. **2** (1969) 65.

27. J. Rodriguez-Carvajal, Fullprof ver. 6.3, *Laboratoire León Brillouin* (CEA-CNRS), France (2018).

28. R. D. Shannon, *Acta Cryst. A* **32** (1976) 751.

29. G. E. Delgado, A. J. Mora, G. Marcano, and C. Rincón, *Mater. Res. Bull*. **38** (2003) 1949.

30. G. E. Delgado, and V. Sagredo, *Bull. Mater. Sci.* **39** (2016) 1631.

31. V. Sagredo, T. E. Torres, G. E. Delgado, and C. Rincón, *Rev. Mex. Fís*. **65** (2019) 14.

32. V. P. Sachanyuk, I. D. Olekseyuk, and O. V. Parasyuk, *Phys. Status sol. (a)* **203** (2006) 459.

33. G. E. Delgado, J. L. Villegas, P. Silva, and V. Sagredo, *Chal. Letters*, **6** (2009) 293.

34. G. E. Delgado, J. A. Flores, P. Grima, M. Quintero, and A. Moreno, *Mater. Res.* **29** (2018) e20160748.